

OP\_Conf.\_2020\_IC-  
STAR\_\_Nasaruddin\_Salam-  
Rustan\_Tarakka\_et.al.pdf  
*by*

---

**Submission date:** 18-May-2023 06:54PM (UTC+0700)

**Submission ID:** 2096185446

**File name:** OP\_Conf.\_2020\_IC-STAR\_\_Nasaruddin\_Salam-Rustan\_Tarakka\_et.al.pdf (893.51K)

**Word count:** 4655

**Character count:** 21433

PAPER · OPEN ACCESS

11

## Flow drags across three minibus car models arranged in tandem in four configurations

7

To cite this article: N Salam *et al* 2021 *IOP Conf. Ser.: Mater. Sci. Eng.* **1173** 012046

View the [article online](#) for updates and enhancements.



**ECS** **240th ECS Meeting**  
Digital Meeting, Oct 10-14, 2021  
**We are going fully digital!**  
Attendees register for free!  
**REGISTER NOW**

The banner features the ECS logo on the left and a photograph of a diverse group of people in a meeting setting on the right. A white diagonal line is overlaid on the photograph.

11

## Flow drags across three minibus car models arranged in tandem in four configurations

N Salam<sup>1</sup>, R Tarakka<sup>1\*</sup>, Jalaluddin<sup>1</sup>, M Ihsan<sup>2</sup>, and M A Jimran<sup>1</sup>

<sup>1</sup> Department of Mechanical Engineering, Hasanuddin University, Makassar, Indonesia

<sup>2</sup> Sekolah Tinggi Teknik Baramuli, Pinrang, Indonesia

\*Email: rustan\_tarakka@yahoo.com

**Abstract.** The purpose of this study was to investigate the drag coefficient of flow on three tandem minibuses in four configurations and to determine the optimum drag coefficient across the three cars. Flow drags measurements have been conducted on a wind tunnel by force balance measurement. The minibus car models with a 1:40 ratio to the originals were constructed from iron material with a thickness of 1 mm. The three minibus cars are arranged in four configuration models where car 1 and car 2 are arranged in series while car 3 position changeable according to the configuration. Each configuration model was treated with 6 changes in the distance of the car to 3, while the distance between car 1 and 2 was constant, with similar 7 levels of treatment of velocities ranging from 8 m/s to 20 m/s. Results show a similar drag coefficient ( $C_d$ ) pattern in all configuration models, where smaller  $C_d$  related to greater velocities and smaller distances of the three cars. Furthermore, at a similar  $Re=49,608$ , the smallest  $C_d$  was obtained in model III ( $C_d=0.78$ ), and followed by model II ( $C_d=0.80$ ), model IV ( $C_d=0.81$ ) and model I ( $C_d=0.84$ ).

**Keywords:** flow drag coefficient, three tandem minibus cars, four configuration models

### 1. Introduction

The flow across three minibuses arranged in tandem is a form of fluid flow applicable in transportation and infrastructure engineering, particularly on expressways. Aerodynamic load is one of the major factors that must be addressed in a design, with special characteristics on tandem objects. Due to coupled interferences of flow around grouped or tandem objects, various interesting and unexpected phenomena can be observed.

When fluids flow through objects, for example, a minibus, energy loss will be developed in the influence of drag forces by either boundary layers or flow separations. In boundary layer terms, drag is a direct viscous effect of tangential stress and is therefore termed as viscous or frictional drag. The latter category is due to the effect of pressure by normal forces and is therefore termed shape or pressure drag, although it can also indirectly be due to viscosity. In avoiding energy losses, a cross-sectional shape of the object should be precisely designed. Interaction of the object with other objects can also be engineered, allowing the air to flow through the object without creating separation and resulting uniform flow beyond the objects. This research is about reducing the drag force in cylinders either single or arranged in tandem with various methods.

A research on the reduction of drag on circular cylinders in airflow has incorporated the installation of disturbance rods embedded on the upstream area before the cylinder, and found out that the flow pattern alterations depend on the diameter, distance, and Reynolds number. Reynolds numbers based on the cylinder diameter were ranging from  $1.5 \cdot 10^4$  to  $6.2 \cdot 10^4$ . The total drag reduction was 63% less when compared to the one of a single cylinder [1].

Research on the efficacy of installing a minute control rod upstream of the cylinder with a focus on the drag and flow pattern has also been conducted, in Reynolds number of approximately  $Re=20,000$ ,



Content from this work may be used under the terms of the Creative Commons Attribution 3.0 licence. Any further distribution of this work must maintain attribution to the author(s) and the title of the work, journal citation and DOI.

based on the diameter of the main cylinder. The highest reduction of the total drag coefficient of the total arrangement consisting main cylinder and control rod has been investigated to approximately 25%. Furthermore, the research was carried out by varying the values of  $L/D$  and  $d/D$ , resulting in total reduction of drag coefficient. From the research, it was also found that the ideal ratio of the diameter of the disturbance rod was at  $d/D=0.233$ . Installation of the minute control rod were ideal in the ratios of distance to cylinder diameter  $L/Ds=2.0-2.08$  [2].

Research on the aerodynamic characteristics of the flow due to the interaction of square cylinders installed in tandem at a laminar flow or low Reynolds number, the eddy flow is affected by the Reynolds number, while the force actions are different between the up-stream cylinder compared to the down-stream cylinder, producing differences drag coefficient value [3].

Research on the interaction of alternately arranged circular and square cylinders installed upstream in the wind tunnel. The distances between the two cylinders were varied with the ratio  $S/d$  from 0 to 10. It was found out that the pressure drop characteristics were influenced by the ratio of the diameters and distances of the two types cylinders ( $S/d$ ). Furthermore, the optimum results were obtained at  $S/d=1.0-1.5$ , indicating the lowest pressure reduction for overall treatments of changes in positions, diameters, and Reynolds numbers [4].

A research on the use of a circular cylinder as a disturbance cylinder before 2 square cylinders in a tandem arrangement conducted. From this study, the optimum ratio of the distances between a disturbance cylinder to the diameter of tandem cylinders ( $L/D$ ) was of 0.43 and the ratio of the disturbance cylinder's diameter to the tandem cylinder's diameter ( $d/D$ ) was of 0.14, where a reduction in the drag coefficient ( $C_d$ ) was obtained by 21.596% [5].

A research on flow characteristics around an array of four circular cylinders near the wall in the laminar boundary layer was carried out by numerical simulation. The pressure distribution across the cylinders and on each cylinder surface was observed at  $L/D=2.7$  ( $L$  was the distance to the centre of each cylinder;  $D$  was the diameter of the cylinder),  $G/D=0.3$  ( $G$  was the distance between the cylinder surface and the wall), with a variation of  $x/D=5, 10$ , and  $21$  ( $x$  is the distance from the leading edge from the wall to the centre of the upstream cylinder) with a Reynolds number of  $1.743 \cdot 10^4$  based on the cylinder diameter. The numerical simulation method employed the 2D Unsteady Reynolds Averaged Navier Stokes (U-RANS) approach and the  $k-\omega$  SST viscous model utilizing FLUENT 6.3.26 software to observe the flow phenomenon around the cylinder. The results of the study indicated that there was an effect of changes in boundary layer thickness to the pressure distribution in each cylinder [6].

Three square cylinders were arranged in series and parallel configurations. Each configuration was given 2 distance treatment models, namely, Model I, where the distance between cylinder 1 and cylinder 2 ( $M$ ) changed while the distance between cylinder 2 and cylinder 3 ( $N$ ) was set fixed at 6 cm, and Model II where  $M$  and  $N$  changed with the same distance. then treated with the same 7 levels of speed ranging from 8 m/s to 20 m/s. Research took place at the Reynolds numbers ( $Re$ ) from 9,395 to 62,634, or laminar flow for external flow. The experimental results showed that the characteristic of the drag coefficient ( $C_d$ ) in the series configuration increases when the distance of three-square cylinders in a tandem arrangement is enlarged, while in the parallel configuration the value of  $C_d$  decreases when the distance is enlarged. The value of  $C_d$  obtained in each of the series and parallel configuration models is smaller than the  $C_d$  value of a single square cylinder [7]. Salam et al. have also investigated flow separation on three tandem square cylinders in serial and parallel configuration [8]. Also, other researchers have defined the value of the drag coefficient of drag for minivan cars to be  $C_d = 0.4$ , and for sedan (passenger car) to be  $C_d=0.3$  [9,10].

## 2. Materials and Methods

This research method is experimental in the form of a wind tunnel, to measure the drag force of fluid flow. Measurement of the flow drag force is done by using force balance measurement. The test objects were 3-piece minibus car models, constituting a car model with a length of 121 mm, a width of 45 mm, a height of 43 mm and a hydraulic diameter ( $D$ ) 44 mm and 1:40 ratio of the model to the prototype. The car models were manufactured from iron material with a thickness of 1 mm. The three minibuses were arranged in four configuration models where the position of car 1 and car 2 was arranged in series at a constant distance  $L$ , while the position of car 3 changes in the Y direction or moving sideward at the distance of  $M$ , and in the X direction or moving forward at a distance of  $N$  depending on the

configuration models, namely the configuration model I (car 3 parallel to car 2 or at  $N/D=0$ ), configuration model II (car 3 parallel in between car 1 and car 2 or at  $N/D=2.75$ ), configuration model III (car 3 parallel to car 1 or at  $N/D=5.5$ ), and configuration model IV (car 3 parallel and ahead to car 1 or at  $N/D=8.25$ ).

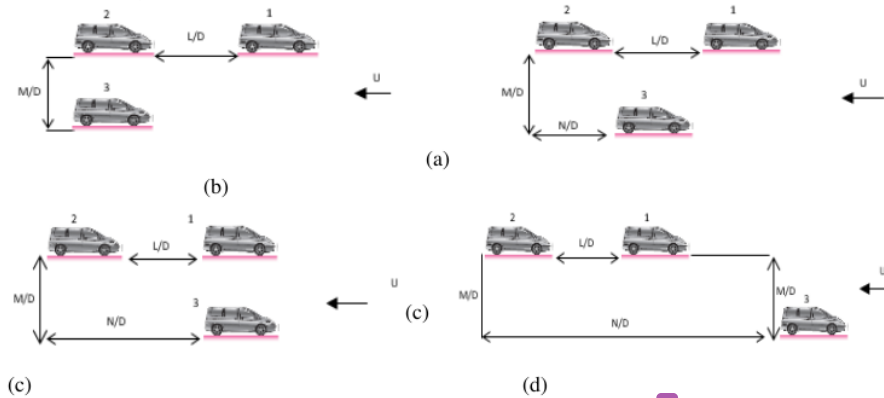


**Figure 1** Tandem positions of 3-minibus in four configuration models (a) configuration model I, (b) configuration model II, (c) configuration model III and (d) configuration model IV

Furthermore, each configuration model was given 6 variations in M distance and 4 variations in N distance from 0.57 to 3.41 with car 2 arranged in series, then given the same 7 levels of speed treatment ranging which were 8 m/s, 10 m/s, 12 m/s, 14 m/s, 16 m/s, 18 m/s and 20 m/s. Figure 1 shows the position of the three minibuses arranged in tandem in four configuration models, with a distance ratio  $M/D$  of 6 levels, (namely, 0.57; 1.13; 1.70; 2.72; 2.84 and 3.41) and the ratios of the distance between  $N/D$  of 4 levels, (namely, 0; 2.75; 5.50 and 8.25) while the ratio of distance  $L/D$  was constant of 2.75.

The equipment was international standard testing equipment in the Laboratory of Fluid Mechanics, Department of Mechanical Engineering, Faculty of Engineering, Hasanuddin University. The wind tunnel used in this study is a low-speed wind tunnel made by Plint & Partners LTD Engineers [10], where the velocity of airflow through the test section (300 mm x 300 mm) is set maximum at 22 m/s. This equipment is equipped with a forces balance measurement equipment and airflow velocity measurement, as shown in Figure 2.



*Remarks:*

1. Prototype Screen;
2. Diffuser;
3. Test section;
4. Divergence section;
5. Fan;
6. Electric motor;
7. Flow velocity measurement;
8. Electric voltage regulator;
9. Force's balance measurement

**Figure 2** Wind tunnel used in the research with its elements [10]

To determine the value of the drag coefficient and describe the characteristics of fluid flow across a minibus, the Reynolds formula was used as shown in Eq. 1 [9],

$$Re = \frac{U \cdot D}{\nu} \quad (1)$$

The variables and parameters in Eq. 1 are the airflow velocity before the test models (U), the hydraulic diameter of the minibus car (D), and the air kinematic viscosity ( $\nu$ ). In determining the drag coefficient ( $C_d$ ), the Eq. 2 was used [9],

$$C_d = \frac{2 \cdot F_d}{\rho_{air} \cdot U^2 \cdot A} \quad (2)$$

The variables in Eq. 2 are the experimental drag force ( $F_d$ ), the frontal surface area of the minibus (A), and the density of the air ( $\rho_{air}$ ). The values of kinematic viscosity and density of air are defined based on the pressure and room temperature in the laboratory.

Based on the hydraulic diameter of the minibus model and the treatment of airflow velocities, ranging from 8 m/s to 20 m/s, or from 28.8 km/h to 72.2 km/h, the experiments were in a laminar flow area or at  $Re < 10^5$  for external flow. Moreover, the flow velocity was maintained in a constant condition at each speed level, and the speed treatments for each configuration model were 7 levels of U velocity, namely (8, 10, 12, 14, 16, 18, and 20) m/s.

### 3. Results and discussion

The experimental results of airflow across three minibuses arranged in tandem in four configuration models show that the characteristics of the drag coefficient ( $C_d$ ) tend to be the same, that is, if the airflow velocity U or the Reynolds number (Re) increases, the  $C_d$  value decreases. The following describes the experimental results for the four configuration models, in the form of a graph of the relationship between  $C_d$  and airflow velocity U or the Re number at the same M/D. The results for four configuration models are subsequently compiled in a graph of the relationship of  $C_d$  and M/D at the same velocity.

The experimental results of the configuration Model I are depicted in Figure 3 in the form of a graph of the relationship between  $C_d$  and Re at the same M/D.

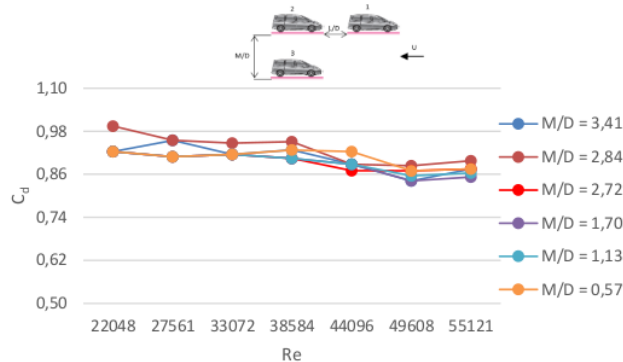


**Figure 3** Relationship of  $C_d$  and Re for configuration model I for 6 levels of M/D and for N/D=0

Based on Figure 3 above, it is shown that the alterations in M/D affects the value of  $C_d$  at all levels of Reynolds numbers. These results show that the largest drag coefficient of  $C_d=0.99$  was at  $M/D=2.84$  and at  $Re=22,048$ , while the smallest resistance coefficient value of  $C_d=0.84$  was at  $M/D=1.70$  and at  $Re=49,608$ . These results indicate that when car 3 is closer to car 2, the flow separation was slowed down causing the boundary layer to shrink, and the vortex of the airflow was dampened at crossing between car 2 and car 3. However, when the position of car 3 is very close to car 2 or at  $M/D=0.57$ , the value of  $C_d$  increases again. The difference in values between the largest and the smallest  $C_d$  shows the effect of changing the distance between car 3 and car 2, and this proves that, in the right position, cars

arranged in tandem in configuration model I can reduce aerodynamic drag. The right position of the car, of course, will result in more efficient fuel consumption.

Figure 4 shows the experimental results of configuration model II, depicting the relationship between  $C_d$  and Re at the same M/D.

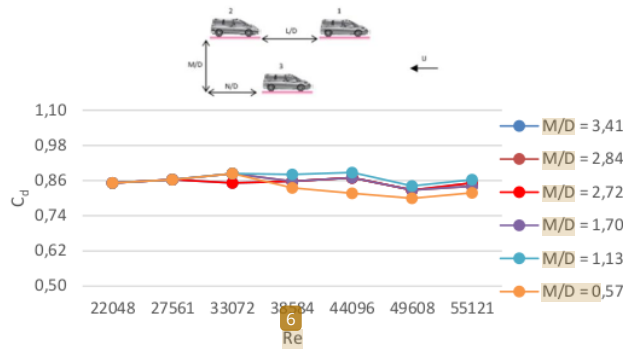


**Figure 4** Relationship of  $C_d$  and Re for configuration model II for 6 levels of M/D and for N/D=2.75

Figure 4 also describes that varying M/D could affect the values of  $C_d$  at all levels of the Reynolds numbers. These results indicate that the largest flow drag coefficient value was  $C_d=0.89$ , occurring at M/D=1.13 and Re=44,096, while the smallest drag coefficient value was  $C_d=0.80$  at M/D=0.57 and Re=49,608. These results indicate that when car 3 is closer to car 2, the flow separation was delaying causing the boundary layer to shrink, and the vortex of airflow was dampened after crossing between car 2 and car 3. The difference of the largest and the smallest  $C_d$  shows the impact if varying the distances between car 3 and car 2, and this also proves that, in proper position, cars arranged in tandem configuration model II can reduce aerodynamic drag which also contribute to the reduction of fuel consumptions.

The same results of configuration model III are shown in Figure 5, which is a graph of the relationship between  $C_d$  and Re at the same M/D.

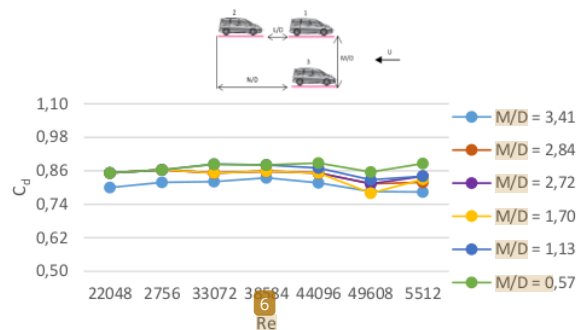


**Figure 5** Relationship of  $C_d$  and Re for configuration model III for 6 levels of M/D and for N/D=5.5

It is also shown in Figure 5 that the changes in M/D have affected the magnitude of  $C_d$  at all levels of the Reynolds numbers. These results also show that the largest flow drag coefficient value was at

$C_d=0.89$  and at  $M/D=0.57$  and  $Re=44,096$ , while the smallest drag coefficient  $C_d$  of  $0.78$  occurred at  $M/D=1.70$  and  $Re=49,608$ . These results also prove that when car 3 is closer to car 1, the flow separation was delaying, resulting on shrunken boundary layer and dampened airflow vortex after the flow passing through the path between car 1 and car 3. The difference value of the largest and the smallest  $C$  shows the effect of altering the side-by-side distances of car 3 to car 1, and this also proves that the car arranged in tandem configuration model III is effective to reduce drag in airflow and of course, will result in savings car fuel consumption.

The experimental results of the configuration model IV is shown in Figure 6 below, as a graph of the relationship between  $C_d$  and  $Re$  at the same  $M/D$ .

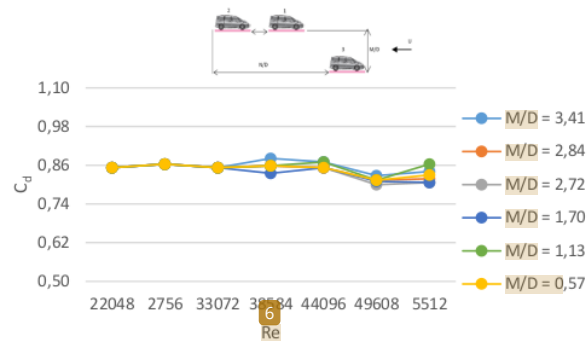


**Figure 6.** Relationship of  $C_d$  and  $Re$  for configuration model IV for 6 levels of  $M/D$  and for  $N/D=8.25$

Figure 6 shows that the change in  $M/D$  will affect the drag coefficient  $C_d$  at all levels of the Reynolds numbers. It gives information that the largest flow drag coefficient was  $C_d=0.88$  at  $M/D=3.41$  and  $Re=38,584$ , while the smallest resistance coefficient value is  $C_d=0.80$  at  $M/D=1.70$  and  $Re=49,608$ . Similar to previous configurations, the results indicate that when car 3 is closer to car 1, the flow separation was again slowed down, resulting the boundary layer to shrink and the vortex of the airflow to dampen after flowing through car 1 and car 3.

The difference in value between the largest and the smallest  $C_d$  shows the effect of changes in the distance between car 3 and car 1, and this also proves that the car arranged in tandem model configuration IV can reduce aerodynamic drag, if set the right position. The expected results is also the reduction fuel consumption.

The compilation results of the four configuration models are shown in Figure 7 below in the form of a graph of the relationship between  $C_d$  and  $M/D$  at the same  $Re=49,608$ .

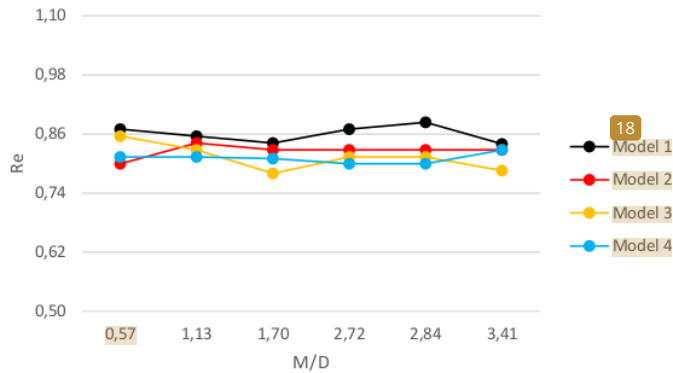


**Figure 7** Relationship of  $C_d$  and  $M/D$  for the four configuration models and for  $Re=49,608$

Based on Figure 7 above, it is indicated that at the same  $M/D$  and  $Re$ , the value of  $C_d$  will be different in different configuration models. Configuration model I shows the value of  $C_d$  which was always greater for all levels of  $M/D$ . The configuration model II, configuration model III, and configuration model IV gave smaller  $C_d$  from the former to the latter. However, at  $M/D=1.70$  the smallest  $C_d$  value was on configuration model III. The same results occurred for  $M/D=3.41$ , where the smallest  $C_d$  value was also occurring in configuration model III.

These results indicate that when car 3 is closer to car 1 and car 2 or at  $M/D=1.7$  the configuration model III is the most optimum one in reducing drag coefficient. This is because the flow separation was slowed down and resulted the boundary layer to shrink. The vortex of airflow was also dampened after crossing between car 1 and car 2 and car 3. Whereas when car 3 was in the farthest position from car 1 and car 2 or at  $M/D=3.41$ , the configuration model III was the best. This is also because the flow separation was slowed down, producing shrunken boundary layer and dampened the airflow vortex after crossing between car 1 and car 3.

The difference in the value between the largest and the smallest  $C_d$  shows the effect of changing the distance of car 3 next to car 1, and this proves that the car is arranged in tandem model configuration IV, which can reduce airflow resistance when in the right position. The right position of the car, of course, will result in savings in car fuel consumption.

The characteristic values of  $C_d$  towards the  $M/D$ s for the four configuration models are as shown in Figure 7 above. The results are then compiled with the CFD flow path line simulation results at  $M/D=1.7$  and  $Re=49,608$ , as shown in Figure 8.

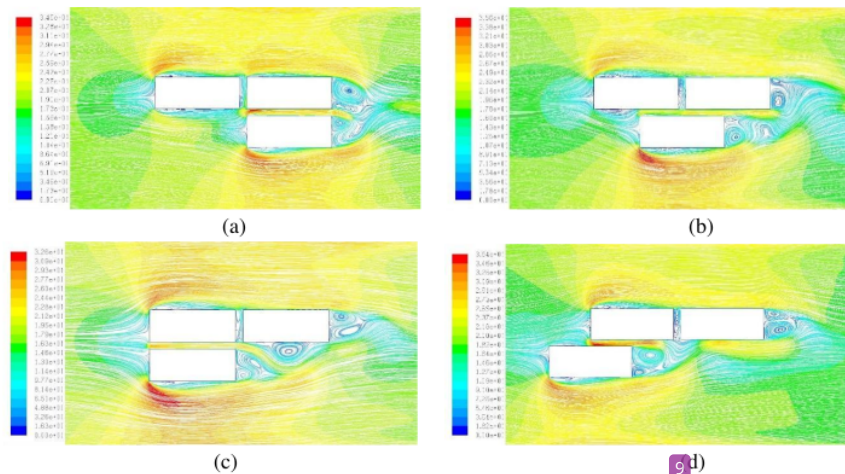


**Figure 8.** Simulated CFD pathlines of flows at  $M/D=1.7$  and  $Re=49608$  for (a) configuration model I, (b) configuration model II, (c) configuration model III, and (d) configuration model IV

Based on Fig. 7 and Fig. 8 above, the best configuration model was configuration model III. This can be seen from the smallest flow vortex that occurs after passing through car 2 and car 3 in configuration model III. The largest flow vortex is in configuration model I. The results of this compilation show conformity to the experimental results. This is because the flow vortex after passing through car 3 in the configuration model III loss its effect on the flow vortex after passing through car 2, creating dampened or more stable flow vortex.

#### 4. Conclusions

It can be concluded that the characteristics of the flow drag coefficient across three minibus cars arranged in tandem in four configuration models have been examined and shows the smallest  $C_d$  value at  $M/D=1.70$  and  $Re=49,608$  or at airflow velocity  $U=18$  m/s (equal to the car speed of 64.8 km/h). An exception is for configuration model II at  $M/D=0.57$ . Also, the smallest drag coefficients of flow across three minibuses arranged in tandem for respective configuration model I, II, III, and IV respectively are:  $C_d=0.84$  at  $M/D=1.70$  and  $Re=49,608$ ;  $C_d=0.80$  at  $M/D=0.57$  and  $Re=49,608$ ;  $C_d=0.78$  at  $M/D=1.70$  and  $Re=49,608$ ; and  $C_d=0.81$  at  $M/D=1.70$  and  $Re=49,608$ . On the condition of the minibus moves independently, the  $C_d$  value for each car was 0.4 resulting total  $C_d$  value of 1.2. Whereas if the three minibuses move in tandem with configuration model I, II, III, and IV, the total average smallest value was  $C_d=0.8075$ , resulting the reduction of  $C_d$  by 31.71%.

#### Acknowledgement

This research was funded by Hasanuddin University Basic Research scheme, 2020 Fiscal Year based on the Unhas Chancellor's Decree Number 2649 / UN4.1 / KEP / 2020, May 22, 2020, managed by the Institute of Research and Community Service, Hasanuddin University.

#### References

- [1] Tsutsui, T. and Igarashi, T. 2002. Drag reduction of a circular cylinder in an air-stream. *Journal of Wind Engineering and Industrial Aerodynamics*, **90**, pp.527-541.DOI: 10.1016/s0167-6105(01)00199-4

- [2] Lee, S., S. Lee, and C. Park 2004, Reducing the drag on a circular cylinder by upstream installation of a small control rod, *Fluid Dynamics Research*, **34**. Pp.233-250. DOI: 10.1016/j.fluidyn.2004.01.001
- [3] Etmian A., Moosavi, M. and Ghaedsharafi, N. 2011. Characteristics of aerodynamics forces acting on two square cylinders in the streamwise direction and its wake patterns, *Advances in Control, Chemical Engineering, Civil Engineering and Mechanical Engineering*. pp. 209-217. DOI: 10.1016/0167-6105(92)90522-c
- [4] Daloglu, A. 2008. Pressure drop in a channel with cylinder in tandem arrangement, *International Communication in Heat and Mass Transfer*, **35**, pp.76-83. DOI: 10.1016/j.icheatmasstransfer.2007.05.011
- [5] Salam, N., Tarakka, R., Jalaluddin, and Bachmid, R. 2017, The effect of the addition of inlet disturbance body (IDB) to flow drag through the square cylinders arranged in tandem, *International Review of Mechanical Engineering (I.R.E.M.E.)*, **11**(3), pp. 181-190. DOI:10.15866/ireme.v11i3.11338
- [6] Wailanduw A. G., Adiwibowo, P. H. and Achmad, H.B. 2018. Numerical simulation of cross flow around four circular cylinders in an in-line square configuration near a plane wall at laminar boundary layer, *Prosiding SNTTM XVII*, pp.162-167.
- [7] Salam, N., Tarakka R., Jalaluddin, Sukardin, M.S., and Machfud, A. 2019. Karakteristik koefisien tahanan aliran melintasi tiga silinder persegi tersusun tandem konfigurasi seri dan paralel. *Prosiding Seminar Nasional Teknik Mesin Politeknik Negeri Jakarta* (2019), ISSN 2085-2762. pp.1244-1251.
- [8] Salam, N., Tarakka, R., Jalaluddin, Ihsan, M. 2020. Flow separation across three square cylinders arranged in serial and parallel tandem configuration. *International Journal on Engineering Applications*, **8**(3), pp. 96-106. DOI: 10.15866/irea.v8i3.18302
- [9] Cengel, Y.A., and Cimbala, J.M. 2006. *Fluid Mechanics Fundamentals and Applications*, Published by The McGraw-Hill Companies, Inc. New York.
- [10] Plint & Partner LTD Engineer. 1982. *Manual Educational Wind Tunnel*, England.

ORIGINALITY REPORT

---

19%

SIMILARITY INDEX

12%

INTERNET SOURCES

17%

PUBLICATIONS

6%

STUDENT PAPERS

---

PRIMARY SOURCES

---

1

Submitted to Aston University

Student Paper

3%

---

2

Syahrir Habiba, Nasaruddin Salam, Rustan Tarakka, Jalaluddin, Muhammad Ihsan.

"Distribution of fluid flow pressure through tandem square cylinders with the addition of triangular cylinder as a disturbance object", IOP Conference Series: Earth and Environmental Science, 2021

Publication

2%

---

3

Nasaruddin Salam, Rustan Tarakka, Jalaluddin Jalaluddin, Reza Bachmid. "The Effect of the Addition of Inlet Disturbance Body (IDB) to Flow Resistance Through the Square Cylinders Arranged in Tandem", International Review of Mechanical Engineering (IREME), 2017

Publication

2%

---

4

Nasaruddin Salam, Rustan Tarakka, Jalaluddin Jalaluddin, Muh. Setiawan Sukardin. "Fluid Flow Resistance Through Hemispherical

1%

Dimpled Plates in Parallel and Zigzag Configurations", International Review of Mechanical Engineering (IREME), 2018

Publication

---

5	<a href="http://hal.sorbonne-universite.fr">hal.sorbonne-universite.fr</a> Internet Source	1 %
6	Syahrir Habiba, Nasaruddin Salam, Rustan Tarakka, Jalaluddin, Muhammad Ihsan. "Effects of the application of inlet disturbance bodies to drag coefficients of tandem arranged square cylinders", AIP Publishing, 2022 Publication	1 %
7	<a href="http://repository.lppm.unila.ac.id">repository.lppm.unila.ac.id</a> Internet Source	1 %
8	<a href="http://ic-star.unila.ac.id">ic-star.unila.ac.id</a> Internet Source	1 %
9	Yin Wang, Lingxin Zhou, Ye Wu, Qing Yang. "New simple correlation formula for the drag coefficient of calcareous sand particles of highly irregular shape", Powder Technology, 2018 Publication	1 %
10	"Fluid Mechanics and Fluid Power – Contemporary Research", Springer Science and Business Media LLC, 2017 Publication	1 %

---

11	<a href="http://www.proquest.com">www.proquest.com</a> Internet Source	1 %
12	T. Tsutsui, T. Igarashi. "Drag reduction of a circular cylinder in an air-stream", Journal of Wind Engineering and Industrial Aerodynamics, 2002 Publication	<1 %
13	Submitted to Adana Bilim ve Teknoloji Universitesi Student Paper	<1 %
14	Submitted to Oklahoma State University Student Paper	<1 %
15	Submitted to University of Surrey Student Paper	<1 %
16	A. Grummy Wailanduw, Triyogi Yuwono. "Numerical simulation of cross flow around four circular cylinders in an in-line square configuration with the critical spacing ratio "L/D" near a plane wall", AIP Publishing, 2018 Publication	<1 %
17	<a href="http://res.mdpi.com">res.mdpi.com</a> Internet Source	<1 %
18	<a href="http://www.canon-igs.org">www.canon-igs.org</a> Internet Source	<1 %
19	<a href="http://www.ijmerr.com">www.ijmerr.com</a> Internet Source	<1 %

20	<a href="http://www.science.gov">www.science.gov</a> Internet Source	<1 %
21	<a href="http://www.wseas.us">www.wseas.us</a> Internet Source	<1 %
22	<a href="http://core.ac.uk">core.ac.uk</a> Internet Source	<1 %
23	<a href="http://dl.icdst.org">dl.icdst.org</a> Internet Source	<1 %
24	<a href="http://livedna.net">livedna.net</a> Internet Source	<1 %
25	<a href="http://resits.its.ac.id">resits.its.ac.id</a> Internet Source	<1 %
26	Mavridou, Sofia G., Efstathios Konstandinidis, and Demetri G. Bouris. "Experimental evaluation of pairs of inline tubes of different size as components for heat exchanger tube bundles", International Journal of Heat and Mass Transfer, 2015. Publication	<1 %

Exclude quotes  On

Exclude matches  < 5 words

Exclude bibliography  On